Activity-based cell sorting reveals resistance of functionally degenerate *Nitrospira* during a press disturbance in nitrifying activated sludge

Maxwell B.W. Madill[1,+], Yaqian Luo[1,+], Pranav Sampara[1], Ryan M. Ziels[1,#]

[1] Department of Civil Engineering, University of British Columbia, Vancouver, Canada

[+] Contributed equally to this work.

[#] Corresponding Author:
Email: ziels@mail.ubc.ca

Running Title: BONCAT-FACS of activated sludge nitrifying microbiomes

Word Count of Abstract: 249
Word Count of Importance: 150
Word Count of Text: 4958

Abstract

Managing and engineering activated sludge wastewater treatment microbiomes for low-energy nitrogen removal requires process control strategies to stop the oxidation of ammonium at nitrite. Our ability to out-select nitrite oxidizing bacteria (NOB) from activated sludge is challenged by their metabolic and physiological diversity, warranting measurements of their *in situ* physiology and activity under selective growth pressures. Here, we examined the stability of nitrite oxidation in activated sludge during a press disturbance induced by treating a portion of return activated sludge with a sidestream flow containing free ammonia (FA) at 200 mg NH_3-N/L. The nitrite accumulation ratio peaked at 42% by day 40 in the experimental bioreactor with the press disturbance, while it did not increase in the control bioreactor. A subsequent decrease in nitrite accumulation within the experimental bioreactor coincided with shifts in dominant *Nitrospira* 16S rRNA amplicon sequence variants (ASVs). We applied bioorthogonal non-canonical amino acid tagging (BONCAT) coupled with fluorescence activated cell sorting (FACS) to investigate changes in the translational activity of NOB populations throughout batch exposure to FA. BONCAT-FACS confirmed that the single *Nitrospira* ASV washed-out of the experimental bioreactor had reduced translational activity following exposure to FA, whereas the two *Nitrospira* ASVs that emerged after process acclimation were not impacted by FA. Thus, the coexistence of functionally degenerate and physiologically resistant *Nitrospira* populations provided resilience to the nitrite-oxidizing function during the press disturbance. These results highlight how BONCAT-FACS can resolve ecological niche differentiations within activated sludge and inform strategies to engineer and control microbiome function.

Importance:

Nitrogen removal from activated sludge wastewater treatment systems is an energy-intensive process due to the large aeration requirement for nitrification. This energy footprint could be minimized with engineering control strategies that wash-out nitrite oxidizing bacteria (NOB) to limit oxygen demands. However, NOB populations can have a high degree of physiological diversity, and it is currently difficult to decipher the behavior of individual taxa during applied selective pressures. Here, we utilized a new substrate analog probing approach to measure the activity of NOB at the cellular translational level in the face of an applied press disturbance to the activated sludge process. Substrate analog probing corroborated the time-series reactor sampling, showing that coexisting and functionally redundant *Nitrospira* provided resilience to the nitrite oxidation process. Taken together, these results highlight how substrate analog approaches can illuminate *in situ* ecophysiologies within shared niches, and can inform strategies to improve microbiome engineering and management.

Introduction

Relating the in situ physiological responses of individual taxa in the face of environmental perturbations to the resulting microbial community structure and function remains a critical challenge for controlling and engineering microbiomes for desirable ecological processes and outcomes (1–3). Biological wastewater treatment processes are ideal ecosystems to explore such relationships, as environmental conditions can be manipulated, and the community function monitored, in a relatively controlled manner (4). A major goal in the wastewater industry is to engineer microbial bioprocesses to achieve energy-efficient, or even net energy-positive, wastewater treatment (5). A foundational component of achieving that goal is the optimization of mainstream biological nitrogen removal processes, as conventionally this process is the largest consumer of energy and exogenous organic carbon within wastewater treatment plants (WWTPs) (6, 7). Realizing energy-efficient nitrogen removal requires highly finessed and sustained modulation of abundances, activities and interactions of key microbial functional groups to effectively control the global community function and engage the desired nitrogen removal pathway(s) (8, 9). As such pathways typically impose inherent energetic and/or metabolic constraints (10, 11), and often challenge existing community interactions (8, 9), it is critical to fully illuminate the ecophysiological diversity and mechanisms driving niche partitioning within those microbial functional groups, as well as their responses to the applied process control strategies (9).

An appealing strategy to achieve energy-efficient biological nitrogen removal is to limit the nitrification process to nitritation (i.e. oxidation of ammonium to nitrite), as the resulting nitrite can be denitrified directly (25% and 40% net energy and carbon reductions, respectively), and/or provided to anammox bacteria as a growth substrate for autotrophic nitrogen removal (60% and 100% net energy and carbon reductions, respectively) (8, 12). However, achieving stable

nitritation in mainstream activated sludge (AS) stands as a major challenge limiting its successful full-scale implementation (13–15). Realizing stable nitritation in mainstream AS relies on engineering control strategies that serve as press disturbances to consistently repress and wash-out nitrite oxidizing bacteria (NOB) while maintaining the activity of ammonium oxidizing bacteria (AOB) (8, 9, 13). The efficacy of a given control strategy is therefore dependent on its ability to create a disturbance that elicits different physiological responses between AOB and NOB. Preliminary success in washing-out NOB from mainstream AS has been achieved using press disturbances that provide a high ammonium residual (13) or control the availability of dissolved oxygen (13, 16, 17) to favour the growth kinetics of AOB over NOB. Additionally, several recently-proposed control strategies have utilized the higher innate sensitivity of NOB to free-ammonia (FA) and free-nitrous acid (FNA) compared to AOB (18–20) to achieve effective NOB inhibition (21–23). Wang et al. (21) demonstrated that a press disturbance induced by exposing a fraction of return sludge to FA-rich sidestream wastewater (210 mg NH_3-N/L) supported successful NOB wash-out in mainstream AS, with nitrite accumulation ratios reaching 80-90%. Despite its potential efficacy for supporting mainstream nitritation, there have been a limited number of studies evaluating the role of niche differentiation and physiological diversity on the stability of nitrite oxidation in the face of a press disturbance from routine FA exposure.

NOB communities in wastewater treatment often display functional degeneracy, wherein the nitrite oxidation process is distributed among several phylogenetically diverse taxa with varying auxiliary metabolic potentials (24–29). Inherent differences in nitrite oxidation biochemistry and cell morphology play core roles in supporting ecophysiological diversity between NOB genera by influencing their substrate affinities for oxygen and nitrite, and their nitrite oxidation kinetics (24, 30, 31). *Nitrospira*, a predominant NOB genus in many WWTP microbiomes (32–34), has demonstrated an extraordinary degree of functional degeneracy, with reports of highly complex and stable communities containing as many as 120 closely-related coexisting strains (26, 27, 34).

Considerable ecophysiological diversity may thus exist between *Nitrospira* species/strains to support niche partitioning, which could be supported by distinct oxygen and nitrite preferences (34–36), auxiliary metabolic potentials for utilizing alternative electron acceptors and/or donors (24, 27, 34, 37, 38), and tolerances to challenging environmental conditions including FA (27, 28, 39, 40). Exhibited at both the genus and strain-level, such functional degeneracy may enable NOB communities to resist the selective pressures imparted by engineering process control strategies by recruiting functionally redundant, yet physiologically diverse, NOB members (41–43). *In situ* assessments of the metabolically active fraction of nitrifying communities are therefore critical to evaluate the efficacy of mainstream nitritation control strategies and elucidate their associated impacts on functionally degenerate NOB.

Next-generation substrate analogue probing approaches have recently emerged as powerful tools to decipher the *in situ* physiology of active cells based on their uptake of synthetic analogues of natural biomolecules (44). Bioorthogonal non-canonical amino acid tagging (BONCAT) is a nascent SAP approach to study the physiology of active cells in complex environmental microbiomes (45–48). BONCAT relies on the *in vivo* uptake and incorporation of synthetic amino acids, such as the alkyne-containing analogue of methionine, homopropargylglycine (HPG), into newly synthesized proteins via the native translational machinery, and thereby selectively labels the proteomes of translationally active cells (44, 47). HPG-labeled cells can subsequently be identified by tagging their proteins with azide-modified fluorescent dyes via azide-alkyne click-chemistry, enabling their selective recovery using fluorescence activated cell sorting (FACS) (45, 46, 48). To our knowledge, BONCAT, or its paired approach with FACS (BONCAT-FACS), have yet to be applied to study the active fractions of AS microbiomes central to wastewater treatment bioprocesses.

The objective of this study was to assess the stability of nitrite oxidation in the face of a press disturbance induced by routine exposure of recycled activated sludge with FA as an engineering control strategy to wash-out NOB. We hypothesized that certain members of the active NOB microbial community could acclimate to the applied press disturbance. Two parallel experimental and control AS sequencing batch reactors (SBRs) were operated for ~100 days to investigate the impacts of routine FA exposure as a press disturbance on the NOB community. We applied time-series 16S rRNA gene amplicon sequencing in addition to BONCAT-FACS based activity measurements to elucidate changes in the structure and *in situ* activity of the AS microbiome and nitrifying communities.

Results

Partial nitritation performance of activated sludge bioreactors

Two AS SBRs treated synthetic mainstream municipal wastewater over two operational phases: the Start-up Phase and the Treatment Phase (Figure S1). Periodic steady-state conditions were presumed over the last 30 days of the 270-day Start-up Phase, during which there were no significant differences in daily effluent concentrations of NH_4^+-N, NO_3^--N, and NO_2^--N between the two SBRs ($p > 0.05$), which averaged 0.1±0.3 mg NH_4^+-N/L, 19±2 mg NO_3^--N/L and 0.0±0.01 mg NO_2^--N/L, respectively (Figure 1). There were also no significant differences in the TSS and VSS of mixed liquor between the two systems during the Start-up Phase ($p > 0.05$; Figure S2). Thus, similar stable performance with full nitrification was achieved in both SBRs during the initial Start-up Phase, indicating effective duplication of operating conditions.

The Treatment Phase was then commenced on day 0 to assess the impacts of a press disturbance induced by routine FA-exposure of return sludge in a side-stream reactor on the nitrifying community structure and activity. Approximately 20% of the return sludge in the

164 treatment SBR was exposed to 200 mg NH_3-N/L as FA at a pH of 9.0 for 24 hrs before being
165 reintroduced into the mainstream SBR on a daily basis, while the same conditions were emulated
166 for the control SBR but without FA added to the side-stream. Additionally, ammonium nitrogen
167 was added (160 mg NH_4^+-N/d) to the control SBR on a daily basis along with the return sludge to
168 achieve equivalent nitrogen loads between the two SBRs. After 10 days of the applied press
169 disturbance, NO_2^--N began to increase in effluent of the treatment SBR, but stayed below
170 detection in the control SBR for the remainder of the Treatment Phase (Figure 1). By day 40,
171 effluent NO_2^--N reached its peak level of 11 mg NO_2^--N/L in the treatment SBR. At the same time,
172 NH_4^+-N accumulated to 3.7 mg NH_4^+-N/L in the treatment SBR between days 37 and 44, yet
173 stayed below 1.2 mg NH_4^+-N/L in the control SBR over the entire Treatment Phase (Figure 1).
174 The accumulation of NO_2^--N in the treatment SBR was transient, however, as the effluent
175 concentration decreased after day 40 and reached a value below detection by day 74 (Figure 1).
176
177 As effluent was sampled from the SBRs on a 24 h basis, and the sidestream return sludge was
178 added once every 24 h, periodic tests were conducted to measure nitrogen species at the end of
179 individual SBR cycles over the course of 24 h to better estimate nitrite accumulation ratios (NARs)
180 (Figure S3). After 20 days of the press-disturbance, the 24 h average NAR was approximately 10
181 times higher in the treatment SBR versus the control (Figure 1C). The NAR reached its peak of
182 41.9% by day 37 in the treatment SBR, aligning with the observed peak in effluent NO_2^--N
183 concentrations. After day 37, the NAR decreased in the treatment SBR, reaching its lowest
184 observed level of 10.9% on day 75. The NAR of the control SBR stayed below 3.2% in the entire
185 Treatment Phase (Figure 1C). This suggests that the nitrite oxidation function was resilient to the
186 press disturbance of routine FA exposure, as the extent of nitrite oxidation inhibition was not
187 sustained after about 40 days.

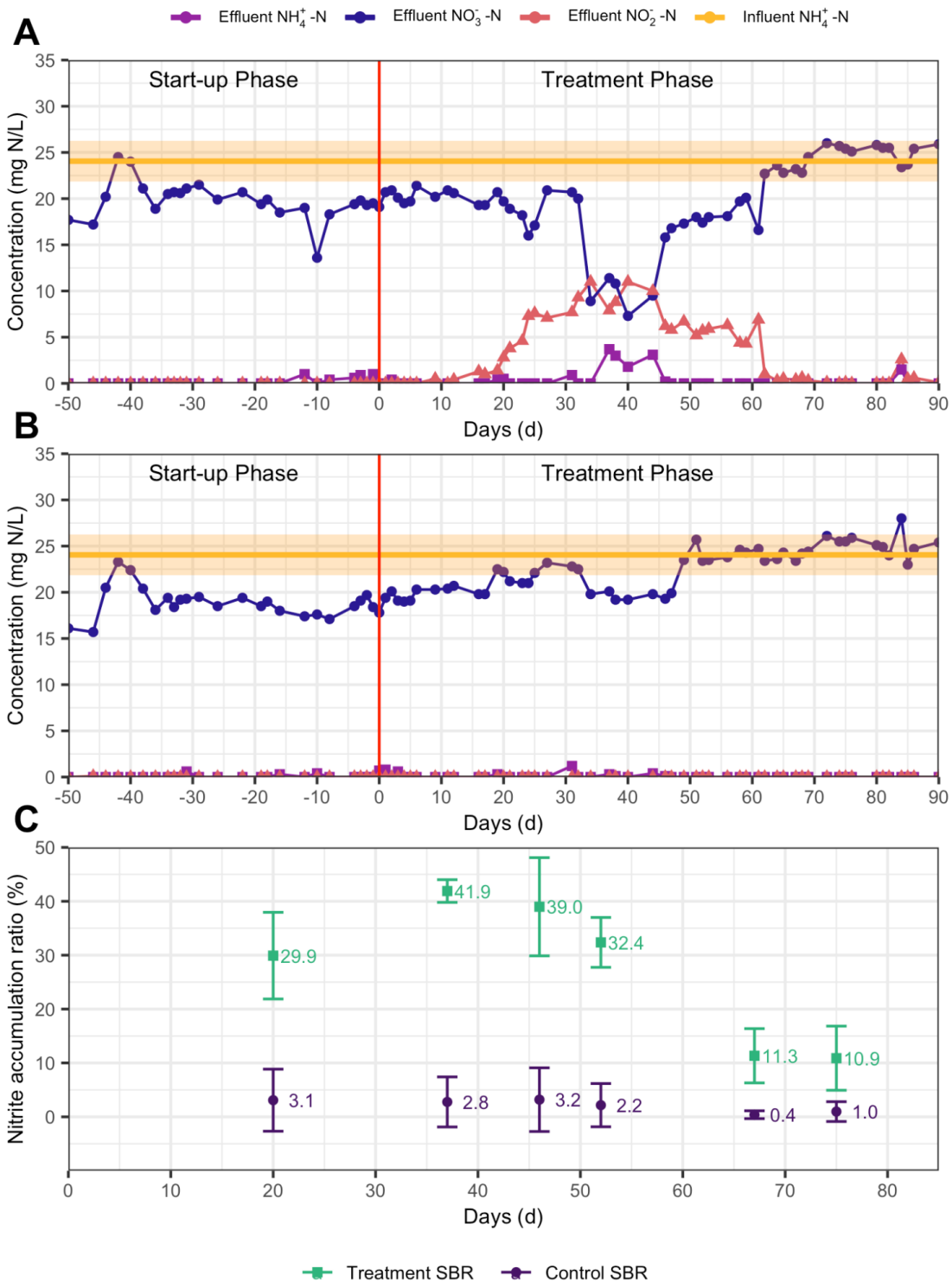

Figure 1: Influent and effluent nitrogen species over the two experimental phases in the (A) treatment sequencing batch reactor (SBR), and (B) control SBR. Shaded orange space represents standard deviation of influent NH_4^+-N. (C) Nitrite accumulation ratio (NAR, %) of treatment and control SBRs over time, based on 24 h monitoring of SBR effluents. NAR is defined

as the effluent nitrite (mg N/L) divided by the effluent nitrite plus nitrate (mg N/L), and indicates the level of NOB activity suppression.

3.2 Microbial community acclimation to routine FA-exposure

Microbial 16S rRNA gene amplicons were denoised into amplicon sequence variants (ASVs) to provide a high-resolution (49, 50) view of how routine FA-exposure impacted the community structure. A total of 3.01 million chimera-free quality-filtered merged reads (Table S1) were denoised into 6,694 ASVs. Over 95% of the 16S rRNA gene amplicons at all time points in both SBRs were comprised of the 8 phyla: *Proteobacteria*, *Bacteroidetes*, *Chloroflexi*, *Nitrospirae*, *Planctomycetes*, *Verrucomicrobia*, *Acidobacteria*, and *Cyanobacteria* (Figure S4). Between 53% to 70% percent of 16S rRNA amplicons were represented by 20 genera across all samples (Figure 2). Even at the broad genus level of resolution, there were apparent differences in community profiles between the treatment and control SBRs over time (Figure 2), indicating that routine FA exposure altered the structure of the AS microbiome.

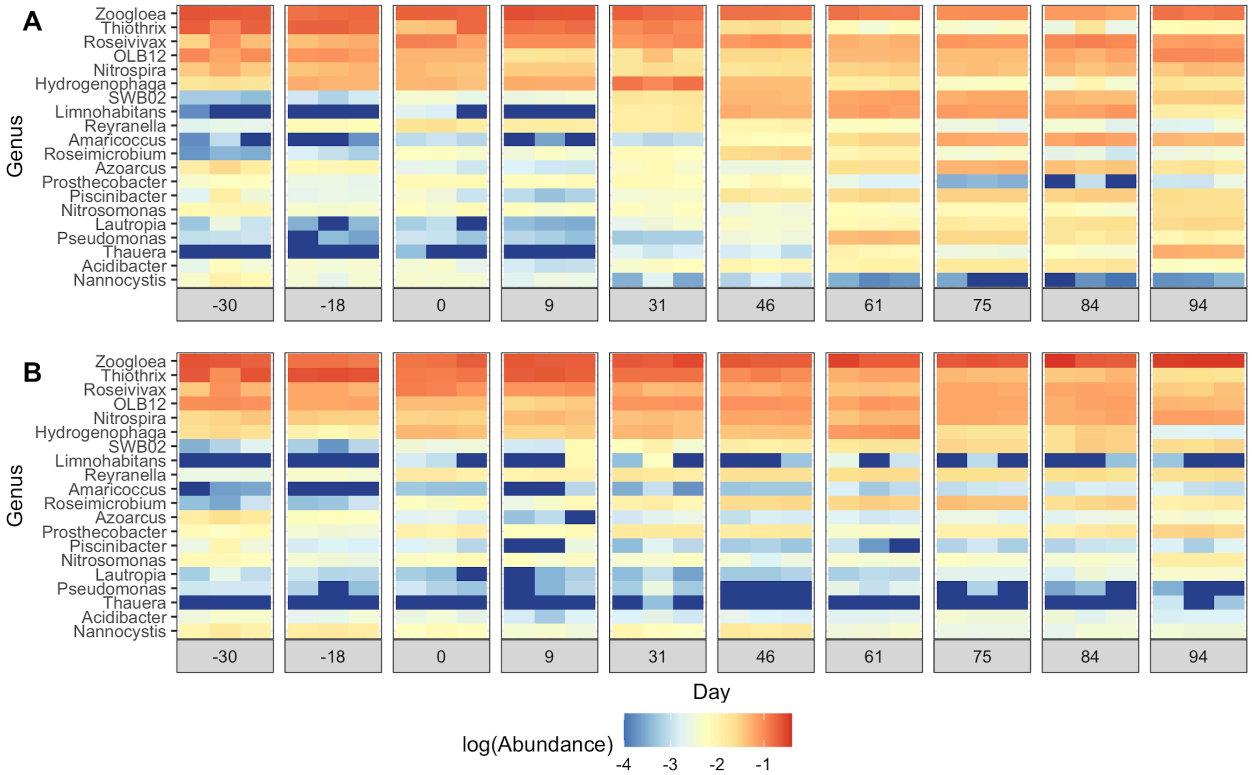

Figure 2: Heatmap of log-scaled relative abundance of top 20 most abundant genera in the (A) treatment SBR and (B) control SBR over the two operational phases. Sequencing results are shown for triplicate DNA extractions on each sampling date. The genera are ordered from highest to lowest cumulative abundance across samples.

At the ASV level, FA-exposure of return sludge led to significant differences in community structure between the two SBRs over time (R^2 = 0.54, p < 0.001, adonis). Principal coordinates analysis (PCoA) of cumulative sum-scaled ASV read counts revealed that community profiles in the two SBRs were similar until day 9, after which the treatment SBR community diverged from the control (Figure 3). Differential abundance analysis showed that there were no statistically different ASVs between the two SBRs on day 0 (p > 0.01, DESeq2), indicating that they were well replicated in the Start-up Phase. By day 46 of the Treatment Phase, around the time that nitrite peaked in the treatment SBR (Figure 1), 105 ASVs spanning 55 genera were differentially abundant between the two SBRs (p < 0.01, DESeq2; Figure S5). The number of ASVs with

224 significant differential abundance between the SBRs continued to increase to a maximum of 166
225 on day 75 of the Treatment Phase (Figure S5).
226

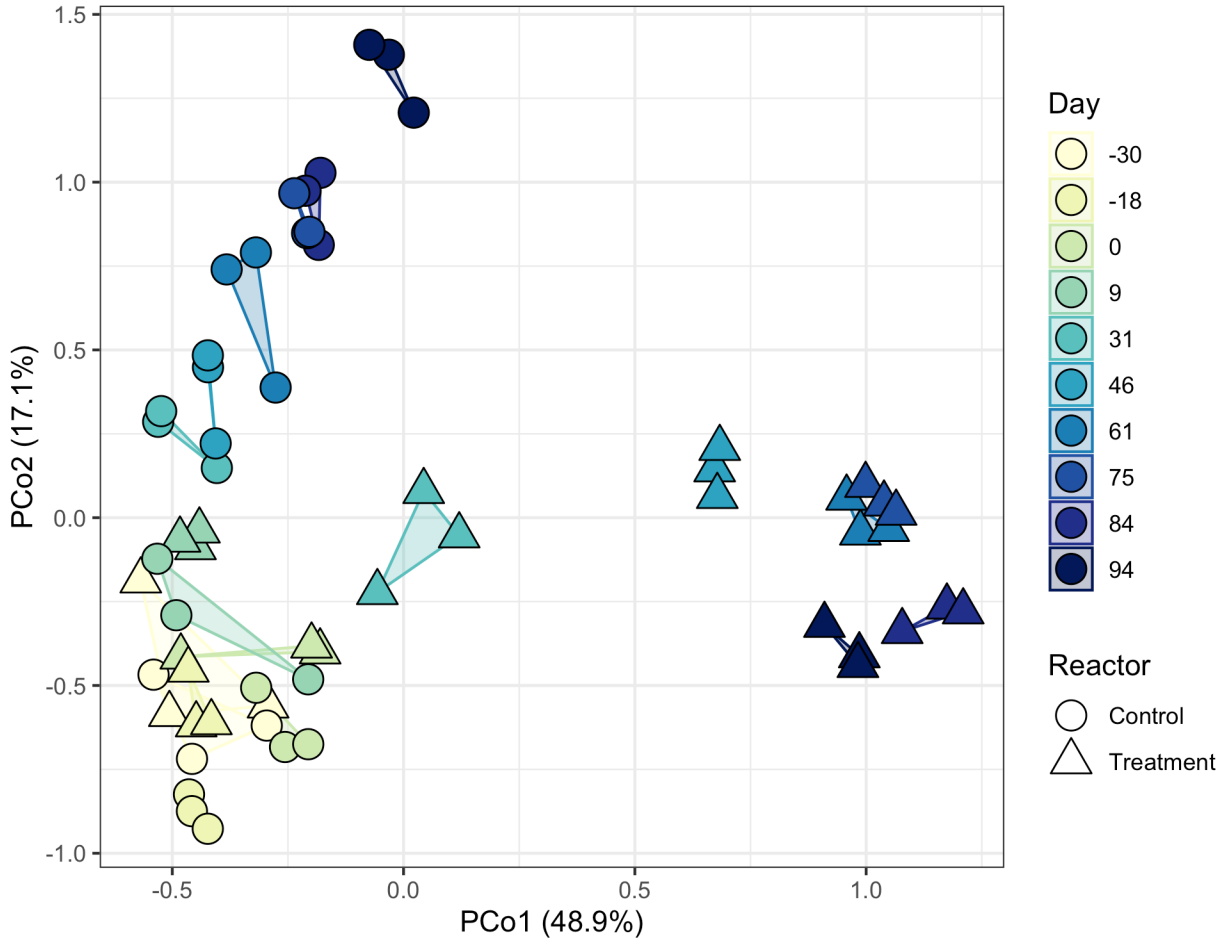

227

228 **Figure 3:** Principal coordinates analysis (PCoA) of Bray-Curtis dissimilarities between cumulative
229 sum scaled (CSS) read counts of 16S rRNA ASVs in both SBRs over time. The marker fill
230 represents reactor operating day, and the marker shape corresponds to the SBR. Triplicate DNA
231 extractions for each time point are indicated by a shared polygon. The percentages in
232 parentheses represent the fraction of variance explained by that axis.
233
234

235 *Nitrospira* and *Nitrosomonas* were the only putative NOB and AOB populations detected in the
236 SBRs, respectively (Figure 2). As these reactors were fed with synthetic wastewater, it is likely
237 that these populations originated from the inoculum. Six dominant *Nitrosomonas* ASVs were

238 detected in both SBRs over the two experimental phases (Figure S6). Until day 84, the total
239 *Nitrosomonas* abundance was less than 1% in both SBRs, but increased to over 1.5% in both by
240 day 94 (Figure S12). One *Nitrosomonas* ASV (ASV_36) was differentially abundant between the
241 two SBRs on days 75 and 94 ($p < 0.01$, DESeq2). Three *Nitrospira* ASVs were detected within
242 the two SBRs (Figure 4). In particular, ASV_8 was the dominant *Nitrospira* ASV in both SBRs
243 during the Start-up Phase (before day 0), accounting for 3.3%±0.8% of 16S rRNA genes on
244 average (Figure 4). By day 46, ASV_8 decreased to 1.6%±0.1% in the treatment SBR, while it
245 increased to 6.4%±0.3% within the control. This decrease in ASV_8 abundance coincided with
246 the peak in nitrite accumulation in the treatment SBR (Figure 1a). The abundance of ASV_8 did
247 not significantly change after day 46 for the remainder of the experiment in the treatment SBR (p
248 > 0.01, DESeq2). In contrast, two other *Nitrospira* ASVs (ASV_32 and ASV_47; 99.7% sequence
249 similarity to each other; 94.2% and 94.5% sequence similarities to ASV_8, respectively) were
250 sporadically detected in both SBRs at abundances below 0.4% until day 46, and then increased
251 to a maximum of 1.8%±0.4% and 1.2%±0.3% in the treatment SBR by day 84, respectively, but
252 stayed below 0.3% in the control (Figure 4). The abundance of ASV_32 and ASV_47 were
253 significantly higher in the treatment SBR relative to the control SBR by the end of the experiment,
254 while ASV_8 was significantly lower (both days 84 and 94; $p < 0.01$, DESeq2). Phylogenetic
255 analysis based on partial 16S rRNA gene sequences (Figure S7) revealed that ASV_8 was most
256 closely related to *Nitrospira lenta* within lineage II, whereas ASV_32 and ASV_47 were clustered
257 within lineage I of *Nitrospira* (51, 52).
258

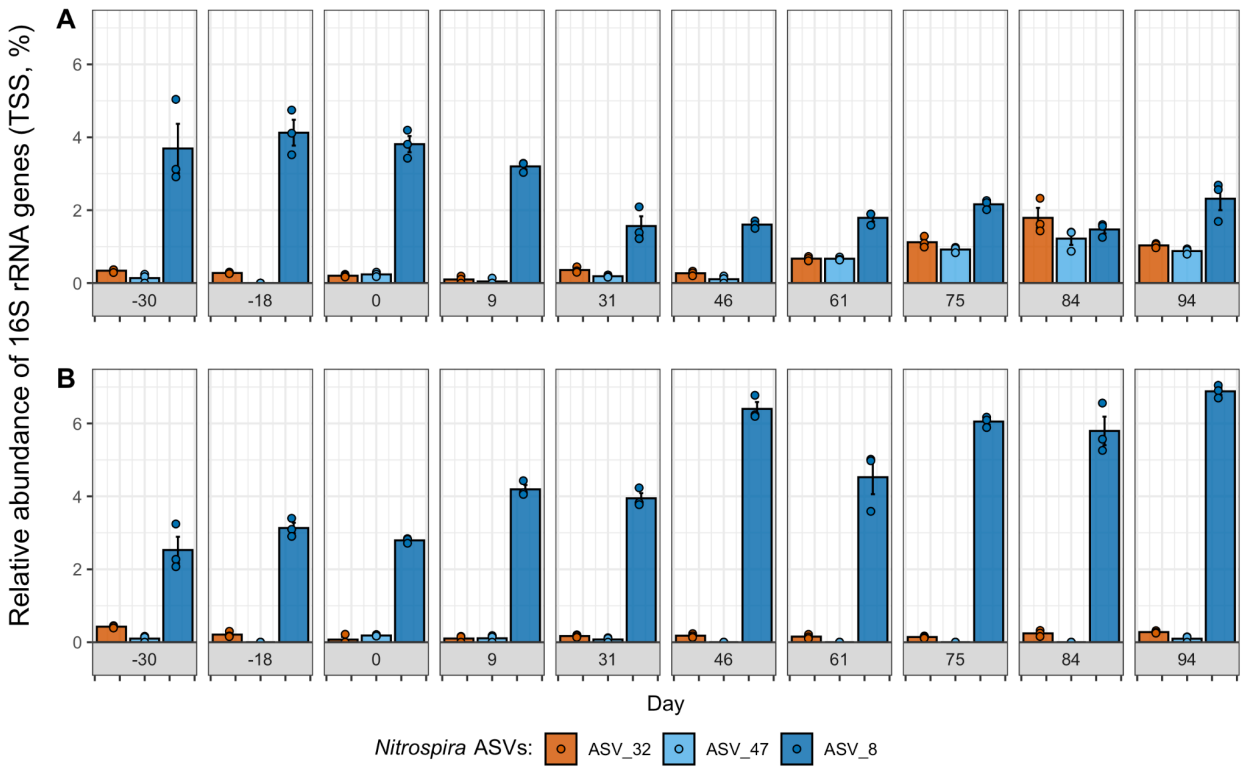

Figure 4: Relative abundance (total sum scaled, TSS) of three dominant *Nitrospira* ASVs over time in the (A) treatment SBR and (B) control SBR. Only *Nitrospira* ASVs detected in more than one sample are shown. Results are shown for triplicate DNA extractions on each day, with the coloured points showing the relative abundance of each ASV in each DNA extraction, the coloured bar showing the mean relative abundance, and the error bars showing the standard error of the mean.

3.3 Substrate analog probing of active nitrifying populations

To decipher the impact of the applied press disturbance on the activity and *in situ* physiology of nitrifying populations within mainstream AS, we conducted BONCAT-FACS on samples collected from nitrifying microcosms seeded with SBR mixed liquor preceding return sludge treatment (R), as well as return sludge from the beginning (15 min after start; S1) and end (24 h after start; S2) of the side-stream return sludge treatment processes for each SBR (Figure 5). Preliminary validation microcosms confirmed the sensitivity of BONCAT in labeling only active cells that had incorporated HPG (Figure S8). Comparison of FACS data between the two SBRs (Figures S9 and S10) revealed that translationally active (i.e. BONCAT+) cell fractions were significantly lower

in the S1 and S2 nitrifying microcosms seeded from the FA-exposed treatment SBR relative to those of the control SBR ($p < 0.05$, t-test), but that no significant difference in BONCAT+ cell fractions was observed in the R microcosms seeded with mixed-liquor preceding sludge treatment. (Figure 5). Within the treatment SBR nitrifying microcosms, the fraction of BONCAT+ cells in the S1 microcosm was 25% lower than that of the R microcosm without FA-exposure, but the this was not significant ($p = 0.078$; Figure 5). No further reduction in the fraction of BONCAT+ cells was observed between microcosms seeded with return sludge from the beginning (S1) and end (S2) of the FA-exposure process (Figure 5). In contrast, the BONCAT+ cell fraction in the microcosm seeded with control SBR return sludge after 24 hrs of its sludge treatment (S2) was significantly higher by 63% compared to that at the beginning of its sludge treatment process (S1; p=0.045; Figure 5).

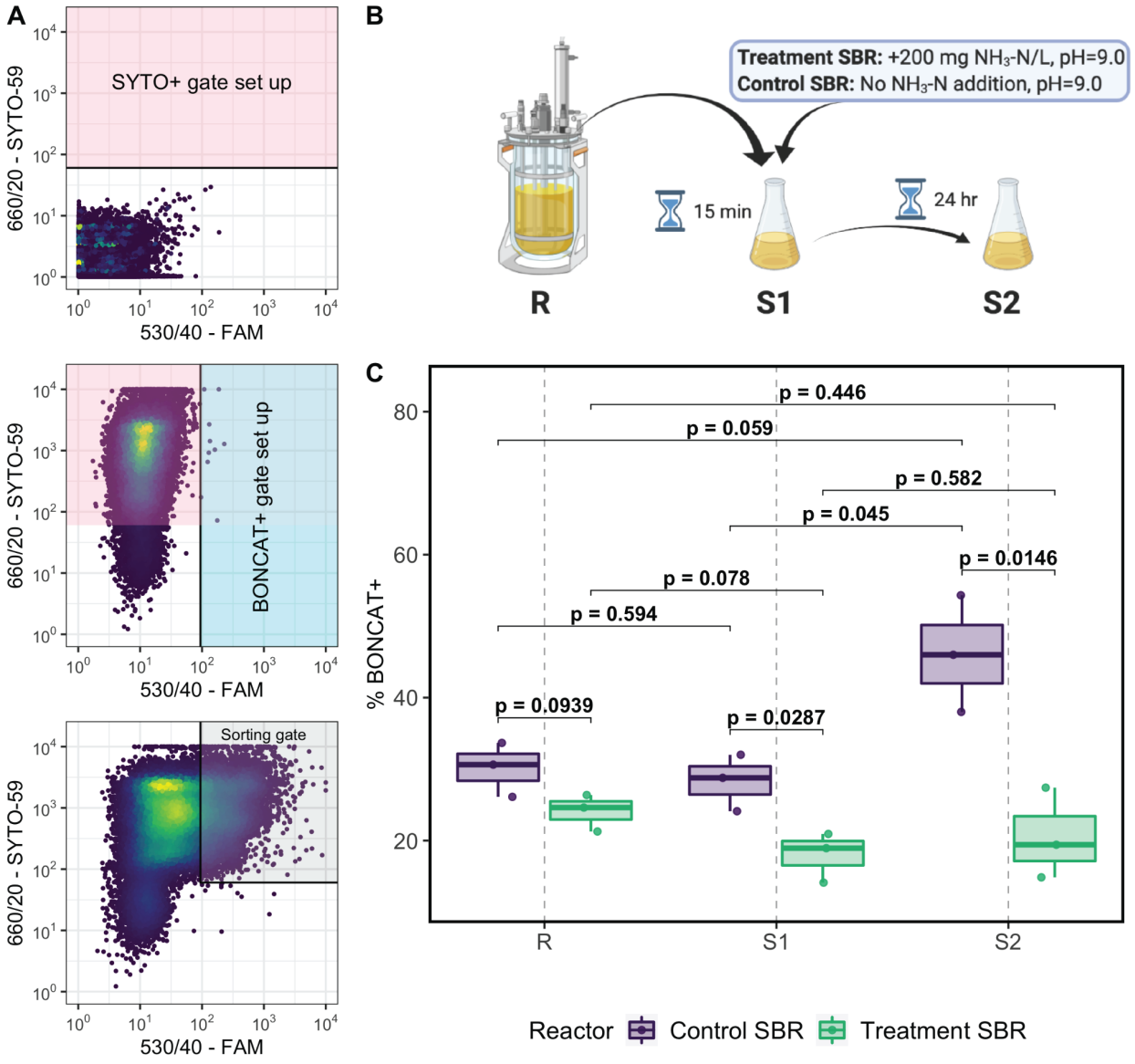

Figure 5: Application of BONCAT-FACS to aerobic nitrifying microcosm samples. (A) Sorting gates were established based on the detection of SYTO+ cells from background particles using unstained HPG-negative cells (top panel), and BONCAT+ cells from non-HPG labelled cells based on their FAM picolyl azide dye fluorescence using SYTO59 stained HPG-negative cells (middle panel), allowing less than 0.5% false positives in each gate. BONCAT+ cell fractions in each HPG-incubated sample were calculated as the fraction of SYTO+ cells residing in the sorting gate (bottom panel). (B) Overview of the return sludge treatment processes showing the origin of samples used to seed the nitrifying microcosms. (C) Comparison of BONCAT+ cell fractions detected in samples prepared from the nitrifying microcosms seeded with mixed-liquor preceding return sludge treatment (R), return sludge after 15 min of side-stream treatment (S1), and return sludge after 24 h of side-stream treatment (S2) from the treatment SBR (bottom) and control SBR (top). Black brackets are shown for comparisons of BONCAT+ cell fractions made between samples, with *p* values calculated using independent t-tests.

304 The microbial community composition observed in the BONCAT+ cell fractions could be attributed
305 to changes in cellular translational activity, as well as any changes that occurred in the bulk
306 community composition throughout the incubation and/or sample processing steps upstream of
307 FACS. To delineate these impacts, we conducted 16S rRNA gene amplicon sequencing on
308 triplicate bulk (i.e. pre-homogenized), post-homogenized and click-chemistry labelled samples
309 from each microcosm, in addition to pre-homogenized bulk samples from HPG-negative control
310 microcosms and SBR mixed liquors prepared with different DNA extraction and PCR amplification
311 procedures. The low-biomass DNA extraction method (prepGEM kit) and the two-step 16S rRNA
312 gene PCR amplification, which were both used to prepare the BONCAT+ libraries, both showed
313 impacts on the community composition relative to respective samples prepared for time-series
314 analysis (i.e. FastDNA Soil kit with one-step PCR; Figure S11). For this reason, the community
315 compositions measured in the BONCAT+ samples were not compared to time-series samples
316 with different DNA extraction and amplification procedures. PCoA revealed that bulk samples
317 from microcosms incubated without HPG were similar to those with HPG, indicating that HPG did
318 not alter the community structure during the 3 h incubation (Figure 6). Bulk samples from the
319 control SBR microcosms (R, S1 and S2) were generally clustered with the mixed liquor sampled
320 directly from the SBR (Figure 6B). In contrast, bulk samples from the treatment SBR microcosms
321 diverged slightly from the bulk SBR community after 24 hrs of FA-exposure (e.g. S2 microcosms;
322 Figure 6A), suggesting that the community composition was altered by exposure to FA. The
323 community compositions of the post-homogenized samples were not identical to the bulk
324 microcosm samples, which could be attributed to cell lysis or the removal of extracellular DNA
325 during the homogenization and click-labeling procedures (45) (Figure 6). Due to the
326 aforementioned findings, the BONCAT+ cell fractions were only compared to their corresponding
327 post-homogenized microcosm samples processed with the same low-biomass DNA extraction
328 method.
329

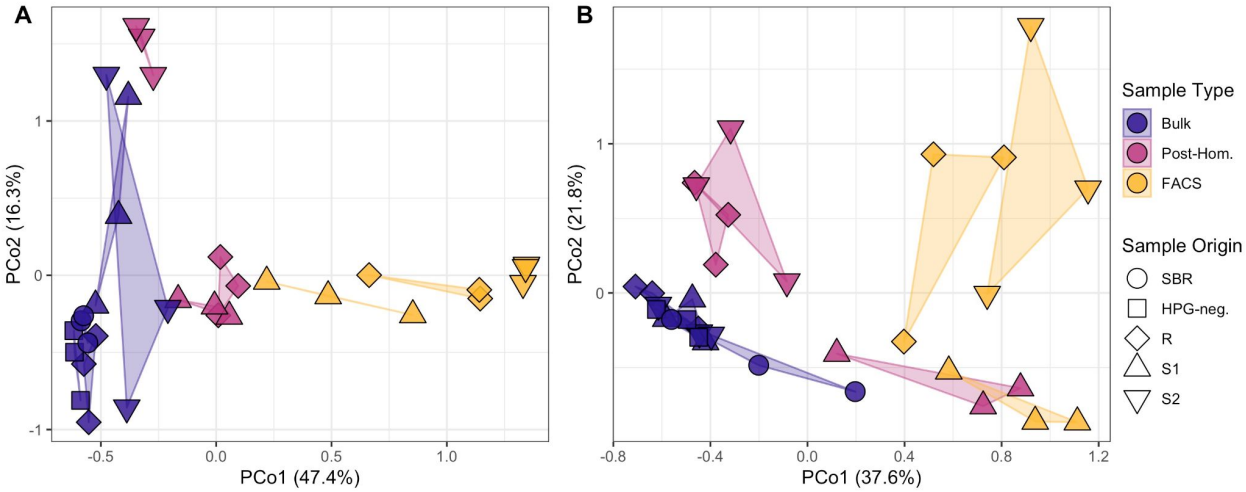

Figure 6. Principal coordinates analysis (PCoA) of Bray-Curtis dissimilarities between cumulative sum scaled (CSS) read counts of 16S rRNA ASVs measured in Bulk, Post-Homogenized (i.e. Post-Hom.) and BONCAT+ (i.e. FACS) samples prepared from nitrifying microcosms seeded with mixed liquor preceding side stream treatment (R), mixed liquor after 15 min of side stream treatment (S1), and mixed liquor after 24 h of side stream treatment (S2), from (A) the treatment SBR and (B) the control SBR. Bulk samples from the HPG-negative R control microcosms (i.e. HPG-neg.) and bulk mixed liquor samples directly from the SBRs (i.e. SBR) were also included. The marker fill represents the preparation procedure for each sample and the marker shape represents the sample origin (microcosm type or SBR mixed liquor). Triplicate samples are indicated by a shared polygon. The percentages in parentheses represent the fraction of variance explained by that coordinate axis.

Comparing the abundance of taxa in a BONCAT+ cell fraction to that in its corresponding bulk community prior to FACS can identify changes in translational activity at the population level (45, 48). For both the treatment and control SBRs, PCoA showed that the largest distance between post-homogenized community compositions and BONCAT+ cell fractions was observed in microcosms seeded with S2 biomass after 24 hrs of FA-exposure (Figure 6). Differential abundance analysis identified 8 and 0 differentially abundant ASVs ($p < 0.01$, DESeq2) in the BONCAT+ fractions of the treatment and control SBR mixed-liquor seeded (R) microcosms, respectively, and 0 differentially abundant ASVs in the BONCAT+ fractions of both SBR microcosms seeded with S1 biomass from the start of return sludge treatment. Conversely, for microcosms seeded with S2 biomass after 24 h of return sludge treatment, 56 and 26 ASVs were differentially abundant in the BONCAT+ fractions of the treatment SBR and control SBR samples,

354 respectively. Within the S2 microcosm BONCAT+ fraction from the treatment SBR, the 56
355 differentially abundant ASVs spanned 26 genera, where 34% of the ASVs were significantly
356 enriched and 66% were significantly reduced, relative to the post-homogenized community
357 (Figure 7). In contrast, the 26 differentially abundant ASVs identified in the S2 microcosm
358 BONCAT+ fraction from the control SBR, which spanned 13 genera, were all (100%) enriched
359 relative to the post-homogenized community (Figure 7). These results suggest that side-stream
360 return sludge treatment caused distinct shifts in the translationally active fraction of the
361 communities in both SBRs, with FA-exposure negatively impacting the activity of a greater
362 number of taxa compared to a similar incubation without FA.

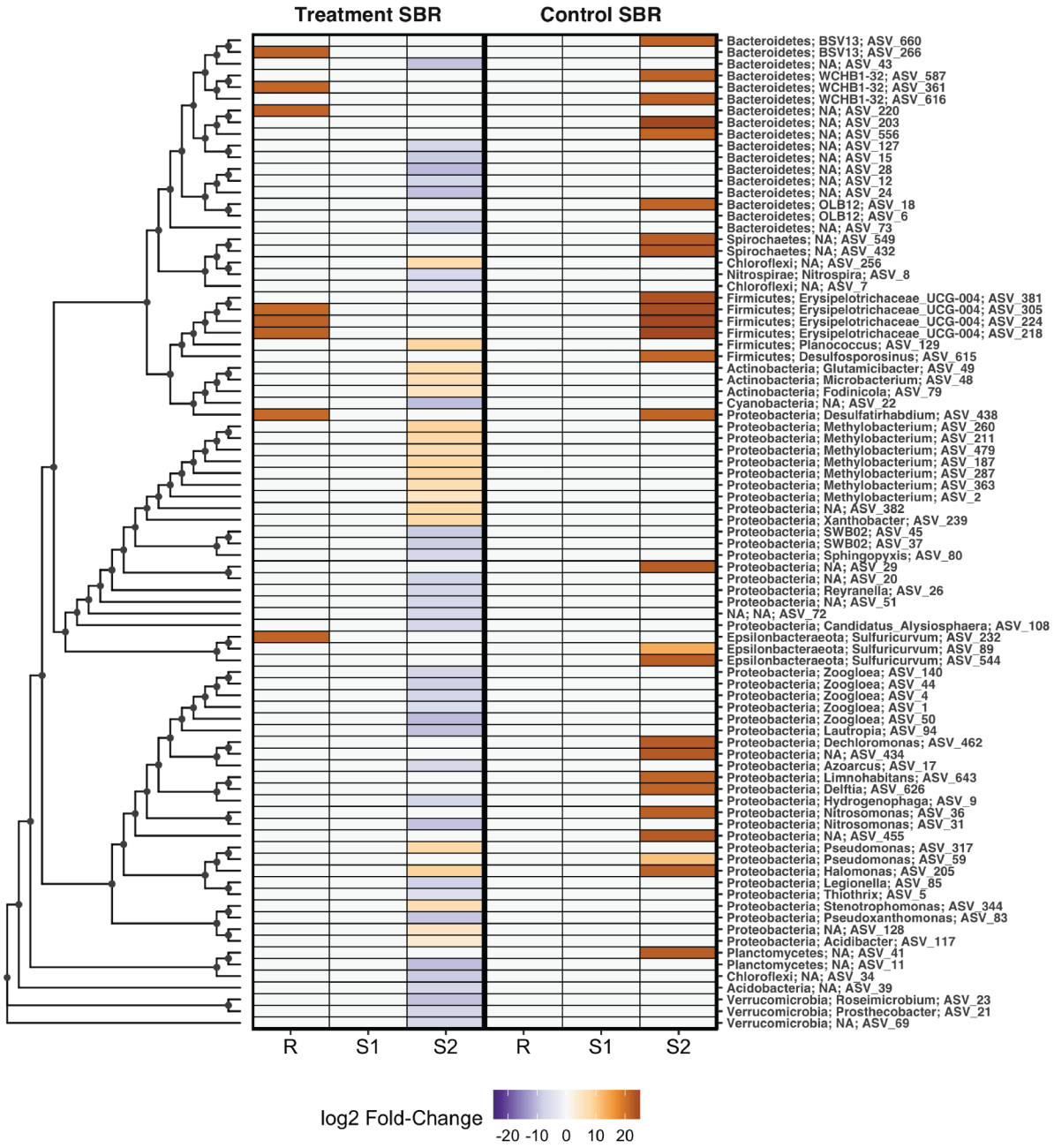

Figure 7: Log_2 fold-change in abundance of all differentially abundant ASVs detected in comparisons between BONCAT+ (i.e. FACS) and Post-Homogenized (i.e. Post-Hom.) fractions prepared from nitrifying microcosms seeded with mixed-liquor preceding return sludge-treatment (R), return sludge after 15 min of side-stream treatment (S1), and return sludge after 24 h of side-stream treatment (S2) from the treatment SBR (left panel) and control SBR (right panel). For each microcosm, log_2 fold-changes are shown only for differentially abundant ASVs, as determined by comparing ASV abundance in triplicate DNA extracts of each fraction using DESeq2 with an adjusted significance level of $p < 0.01$. Log_2 fold-changes that were not significant are set to '0' for visualization purposes. ASVs are ordered based on their phylogenetic distances estimated through multiple sequence alignment using the DECIPHER package (v.2.14.0) (53), and the phylogenetic tree was constructed using a maximum likelihood approach in the phangorn package

(v.2.5.5) (54) in the R environment. Tree tip labels (right side of the heatmap) denote the phylum and genus level classifications of each ASV, where NA denotes an unknown taxonomic identity at that level.

As the BONCAT microcosms were amended with NH_4^+-N as the sole electron donor, it was possible to assess the impact of return sludge treatment on the translational activity of nitrifying populations. The three dominant *Nitrospira* ASVs and the top two dominant *Nitrosomonas* ASVs detected in both SBR BONCAT microcosm sample sets corresponded to the same dominant ASVs detected within both SBR mixed liquors on day 94 of the time-series sampling, when the microcosms were established (Figure 8, Figure S12). The two dominant *Nitrosomonas* ASVs (ASV_31 and ASV_36) were both differentially abundant in the BONCAT+ fractions of S2 microcosms ($p < 0.01$, DESeq2; Figure S12), while the observed differences varied by SBR. *Nitrosomonas* ASV_31 was significantly reduced in the BONCAT+ fraction of the S2 microcosm from the treatment SBR, while *Nitrosomonas* ASV_36 was significantly enriched in the BONCAT+ fraction of the S2 microcosm of the control SBR (Figure S13). Similar to *Nitrosomonas*, the only significant differential abundance in BONCAT+ fractions for *Nitrospira* ASVs occurred in a S2 microcosm (Figure 8). *Nitrospira* ASV_8 was the only differentially abundant NOB in BONCAT+ fractions of both SBR microcosms, and was significantly reduced in the S2 microcosm of the treatment SBR ($p < 0.01$, DESeq2). These results indicate that significant reductions in translational activity of nitrifying populations were only observed in return sludge exposed to FA.

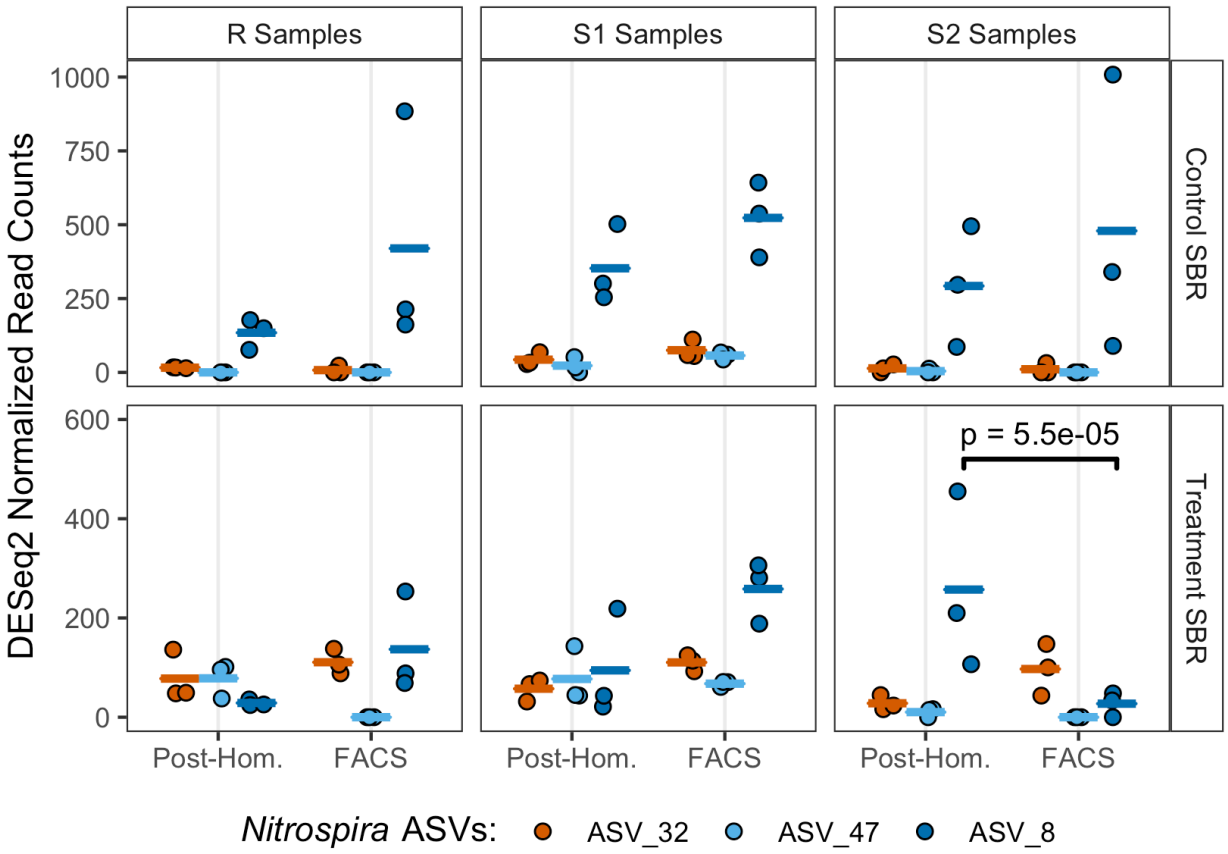

Figure 8: Normalized read counts of three dominant *Nitrospira* ASVs in triplicate BONCAT+ (i.e. FACS) and corresponding Post-Homogenized (i.e. Post-Hom.) and BONCAT+ (i.e. FACS) libraries generated from samples prepared from nitrifying microcosms seeded with mixed-liquor preceding return sludge treatment (R), return sludge after 15 min of side-stream treatment (S1), and return sludge after 24 h of side-stream treatment (S2) from the treatment SBR (bottom) and control SBR (top). Points indicate triplicate normalized read counts per ASV, and the horizontal bars of the same colors represent the sample mean per ASV. The reads were normalized with DESeq2 based on total read-counts per sample. A black bracket between an ASV within two samples represents a significant difference in the mean read abundance, determined with DESeq2 at an adjusted significance level of $p < 0.01$.

Discussion

Implementing process control strategies that achieve consistent modulation of key functional groups remains a critical challenge towards the development of sustainable wastewater treatment biotechnologies. This is particularly true for repressing functionally diverse NOB to promote nitritation for energy-efficient biological nitrogen removal in AS processes. This study

412 demonstrates how underlying shifts in the abundance of physiologically diverse *Nitrospira*
413 populations can confer resilience to the nitrite-oxidizing community during an imposed press
414 disturbance in AS treatment, in this case induced by routine exposure of return sludge to FA. Our
415 results also demonstrate the utility of substrate analog probing approaches like BONCAT to
416 illuminate the *in situ* ecophysiology of shared niches within the activated sludge microbiome, and
417 the associated impacts on process and ecosystem functional stability.
418
419 We observed that routinely exposing ~20% of the return sludge to FA (200 mg NH_3-N/L) in a
420 sidestream reactor with a 24 hr retention time initially reduced nitrite-oxidizing activity in the
421 mainstream reactor, achieving a maximum observed NAR of 42%. However, we observed
422 acclimation of the nitrite-oxidation function after approximately 40 days of the press disturbance,
423 indicated by decreasing NARs within the treatment SBR. This finding is in contrast to those
424 reported by Wang et al. (21) who observed stable repression of NOB activity for over 100 days
425 using a press disturbance of routine FA-exposure at similar conditions (210 mg N/L of FA for 24
426 hr, 22% return sludge exposed). It is important to note that both the pH of the side-stream sludge
427 treatment incubation, and the daily input of total ammonia nitrogen into the mainstream SBR with
428 the return sludge, were controlled across both SBRs. Furthermore, while salinity has been shown
429 to be a driver of Nitrospira population structure (55), the salinity in the side-stream reactor during
430 FA-exposure (~2.5 g/L as Na^+ + Cl^-) was 10-times less than the 50% inhibition level observed for
431 a *Nitrospira* dominated AS community of 30 g/L NaCl (56). Therefore, the inhibition and
432 acclimation of NOB activity to the applied press disturbance can likely be attributed to varying
433 physiological responses of NOB community members to FA-exposure.
434
435 While acclimation of NOB communities in mainstream AS to routine FA-exposure has been
436 previously reported (41, 42, 57), very few studies have directly investigated the role of
437 physiological diversity between NOB members in supporting community-level acclimation. To our

438 knowledge, all previous reports of NOB community acclimation to return sludge FA-exposure
439 have involved shifts in major NOB genera during this press disturbance. Specifically, Li et al. (42)
440 found that *Candidatus* Nitrotoga replaced *Nitrospira* as the dominant NOB in response to return-
441 sludge FA-exposure, while Duan et al. (41) reported a shift from *Nitrospira* to *Nitrobacter* in
442 response to FA-exposure. These reported shifts could be supported by potentially distinct
443 physiological characteristics of *Candidatus* Nitrotoga and *Nitrobacter* compared to *Nitrospira*,
444 such as higher tolerances to FA-inhibition (42, 58) and/or preferences for higher nitrite
445 concentrations (30, 59). In contrast to these genus-level community shifts however, we observed
446 that NOB community acclimation to FA-exposure could occur via shifts between *Nitrospira*
447 sequence variants, specifically from a dominant variant belonging to *Nitrospira* lineage I (ASV_8)
448 to two variants that belonged to *Nitrospira* lineage II (ASV_32 and ASV_47). These findings
449 therefore reveal that physiological diversity at the lineage level, and possibly at the sub-lineage
450 or strain level, within *Nitrospira*-dominated communities can facilitate niche-partitioning and
451 acclimation to FA-exposure as a press-disturbance when applied as an engineering control
452 strategy to promote low-energy nitrogen removal.
453
454 *Nitrospira* species are well-known to be metabolically versatile, with a wide range of functional
455 potentials including nitrite oxidation, hydrogen oxidation, urea conversion, formate oxidation,
456 nitrate reduction, and complete ammonium oxidation (24, 37, 38, 52, 60). This metabolic diversity
457 likely creates opportunities for functionally degenerate *Nitrospira* populations to co-exist within a
458 bioreactor by differentiating in niche space through auxiliary metabolic specializations, while also
459 sharing a common niche space of nitrite oxidation (34, 61). Here, we employed BONCAT-FACS
460 for the first time in an AS wastewater treatment system, to the best of our knowledge, which
461 highlighted differing *in situ* physiologies of three *Nitrospira* variants and resolved their responses
462 to FA-exposure on the level of cellular translational activity. BONCAT-FACS revealed that
463 transitional activity in *Nitrospira* ASV_8 was significantly reduced following exposure to FA for 24

h, aligning with the results of the time-series reactor sampling in which *Nitrospira* ASV_8 was washed out of the treatment SBR but remained dominant in the control SBR. In contrast, *Nitrospira* ASV_32 and ASV_47 increased in abundance within the treatment SBR coinciding with the decrease in NAR after day 40, and BONCAT-FACS revealed the translational activity of those variants remained unchanged following FA-exposure. Based on the close alignment of the BONCAT-FACS observations with the trends in the time-series reactor sampling, it can therefore be hypothesized that the wash-out of *Nitrospira* ASV_8 occurred due to its decreased activity in response to the press-disturbance of routine sidestream FA-exposure, which induced a growth lag once it was reintroduced into the mainstream SBR. In contrast, the potentially distinct auxiliary metabolic potentials of *Nitrospira* ASV_32 and ASV_47 may have conferred their physiological resistance to the side-stream FA-exposure, thereby providing these variants with a competitive growth advantage within the mainstream SBR. Physiological tolerance to FA-exposure was identified as a mechanism of niche-partitioning between *Nitrospira* populations of lineages I and II by Ushiki et al. (40), who showed that *Nitrospira* sp. ND1 of lineage I was more sensitive to FA compared to *Nitrospira japonica* of lineage II at 100 mg NH_4^+-N/L and pH 8.0. Here, we observed that *Nitrospira* ASV_32 and ASV_47 of lineage I were physiologically more tolerant to FA compared to *Nitrospira* ASV_8 of lineage II, suggesting that either lineage-specific tolerances are distinct at the higher FA concentration applied here (200 mg NH_3-N/L) or that physiological tolerance to FA is a trait that varies at the strain/species level within *Nitrospira*. Regardless, once *Nitrospira* ASV_32 and ASV_47 grew to high enough abundances in the treatment SBR, they likely contributed to the net oxidation of nitrite and the decrease in the NAR that was observed after day 40 of the Treatment Phase. Therefore, the FA-exposure press disturbance strategy employed in this study acted as a selective pressure that impacted the stability of the NOB community composition, and functional degeneracy within the *Nitrospira* sequence variants likely provided the nitrite-oxidizing community with resilience by shifting activity to physiologically resistant community members.

The above results highlight the need to combine press disturbances that target the distinct physiological traits of multiple functionally degenerate NOB populations, defined at both the inter and intra genus level, to effectively reduce the aggregate activity of the NOB community for energy-efficient nitrogen removal. For example, if future studies support our finding that lineage I *Nitrospira* are more tolerant to FA than those of lineage II, then combining press-disturbances that further target the physiological traits of lineage I *Nitrospira* along with FA-exposure could prove efficacious. Such strategies could entail the maintenance of high dissolved oxygen concentrations, based on adaptation of lineage I *Nitrospira* to low dissolved oxygen environments (34, 36), or the maintenance of low nitrite concentrations based on their preference for higher nitrite concentrations (34, 40, 51). Measurements of maximal growth rates for these sequence variants could also inform wash-out strategies based on limiting the solids retention time (SRT) (13). Acknowledging the potentially tight tolerances and dynamic nature of nitrite, oxygen, and SRT controls required to target the biokinetics of lineage I *Nitrospira* in full-scale AS systems, combinatorial press-disturbance strategies would likely benefit from control strategies that incorporate frequent community monitoring and biokinetic data of these physiologically diverse NOB populations. These findings also underscore the need for broader applications of *in situ* physiology approaches for elucidating the impacts of NOB out-selection strategies on functionally active NOB members within activated sludge systems.

Accurately measuring the active biomass fraction in microbial bioprocesses is critical, as many key biokinetic models and process mass balances are based on active biomass concentrations (62). However, conventional indirect approaches for quantifying active biomass based on net substrate utilization and growth yields are unable to resolve the compositional and functional dynamics of active microbial populations. As enzymes are the key catalysts that drive the majority of substrate transformations in microbial bioprocesses, we posit that measures of active biomass

should be based on the translationally active microbial cell fraction. The translationally active cell fractions in both SBR microcosms seeded with mixed liquor measured by BONCAT-FACS (R; 24.1% ± 2.6% in treatment, 30.1% ± 3.8% in control) were less than the active biomass fraction predicted through steady-state modeling (63) (67-77% VSS-basis; Supplemental Information), which is likely because the microcosms were only supplemented with ammonium as an electron donor. Nonetheless, we observed many translationally active heterotrophs in the BONCAT microcosms, which could have remained active through metabolism of internal carbon reserves, endogenous respiration, or constitutive protein expression. The consistent increase in translational activity across all differentially abundant ASVs detected in the BONCAT+ fraction of the control SBR microcosm seeded with sludge following the 24 h sidestream incubation could thus have been attributed to fermentative metabolism on cell decay products. In contrast, the mixed translational responses of differentially abundant ASVs in the BONCAT+ fraction of the treatment SBR microcosm following sidestream incubation with FA suggests that more complex dynamics between cellular inhibition, decay, and fermentative metabolism were induced by FA-exposure. This analysis highlights the value of BONCAT as an *in situ* physiology approach to directly measure concentrations of translationally active population members in a microbial bioprocess. This approach could therefore be extended to provide actual measurements of the active biomass concentration for use in calibrating and validating higher-resolution process models, which have been called for as tools to optimize energy-efficient nitrogen removal technologies (9) as well as to better resolve biogeochemical cycles in natural ecosystems (64, 65). BONCAT-FACS could also be extended to resolve associations in the activity of AS taxa with different substrate preferences (48), thus helping to validate ecological-scale models of the wastewater microbiome (66). Therefore, *in situ* physiology approaches like BONCAT show great promise to help inform new strategies to model, control, and engineer microbiome function in both environmental biotechnologies and natural ecosystems alike.

Materials and Methods

Reactor setup, operation and monitoring

Two identical lab-scale sequencing batch reactors (SBRs) with working volumes of 4.28 L were seeded with AS from a pilot-scale SBR at a WWTP in King County (Washington, USA) (Figure S1). The SBR cycles lasted 3 h, including 2 min aerobic feeding, 148 min aerobic reaction, 20 min settling, 5 min decanting, and 5 min idle periods. The SBR cycle timing was controlled with ChronTrol XT timers (ChronTrol Corporation, USA), and mixing was provided by overhead mixers. Reactor temperature was maintained at 20 ± 1 ^{o}C using an environmental chamber. The target solid retention times (SRTs) were kept at 10 days for both SBRs throughout the study by wasting a determined amount of biomass based on daily values of total suspended solids (TSS) and volatile suspended solids (VSS) measured in the mixed liquor and effluent streams. The SBRs were fed with a synthetic wastewater containing ammonium chloride as the nitrogen source and sodium acetate and propionic acid as organic carbon sources, producing 24.5 ± 2 mg NH_4^+-N/L and 100 ± 37 mg/L of soluble chemical oxygen demand (sCOD), respectively, to reflect a sCOD/NH_4^+-N ratio of ~4.0 typical of North American wastewaters (63). Macro and micro element components of the synthetic wastewater are detailed in the Supplemental Information.

Two operational phases were sequentially conducted: the Start-up Phase and the Treatment Phase. In the Start-up Phase, the two SBRs were operated under the same aerobic conditions without FA-exposure of return sludge to achieve similar nitrification performance. The SBRs were fed with 1.07 L of synthetic wastewater in each SBR cycle using peristaltic pumps (LabF1/YZ1515, Shenchen Precision Pump, China), resulting in a hydraulic retention time (HRT) of 12 h. The pH was not controlled but measured within the range of 6.7-7.5. Aeration was provided by an air pump and dissolved oxygen was not controlled, but ranged from 3-8 mg/L in a typical SBR cycle for both reactors. The Start-up Phase lasted 274 days to establish steady-state conditions.

The Treatment Phase was commenced on day 275, hereafter referred to as 'day zero', and lasted 94 days. The operational conditions in the Treatment Phase were similar to those in the Start-up Phase, except for the following differences (Figure S1). In the Treatment Phase, 800 mL of mixed liquor was removed from each SBR at the end of the reaction period of a given cycle every 24 h, and was thickened to 50 mL by centrifugation. The thickened return sludge (50 mL) was incubated in an unstirred 200 mL beaker along with 100 mL of media with the same composition as the synthetic feed, but with no COD. For the experimental reactor, termed the treatment SBR, the return sludge treatment solution contained 1060 mg/L NH_4^+-N, with pH adjusted to 9.0 using sodium hydroxide to produce a final FA concentration of 200 mg NH_3-N/L. These FA and total ammonia nitrogen concentrations are within the range observed in anaerobic digester centrate, particularly co-digestors and those with thermal-hydrolysis pre-treatment (67, 68). In the other reactor, termed the control SBR, thickened return sludge was incubated in the same medium at a pH of 9.0 but without ammonium addition. After 24 h of incubation, the 150 mL of treated return sludge was recycled back into the respective SBRs at the start of the next cycle. To maintain consistent nitrogen loadings in the two SBRs, 0.406 g of ammonium chloride was added to the control SBR simultaneously with the treated return sludge. Monitoring experiments lasting 24 h were performed approximately every 10 days to measure composite daily nitrite accumulation ratios (NARs), as described in the Supplemental Information.

During the Treatment Phase, effluent nutrient samples were collected just before the addition of treated return sludge. Nitrogen species (ammonium, nitrite, and nitrate), orthophosphate, and soluble COD (sCOD) in effluent samples were monitored three to four times per week. pH and DO were measured at least three times per week. Analytical methods for bioreactor monitoring are described in Table S2.

Microcosms for bioorthogonal non-canonical amino acid tagging (BONCAT)

Three 30 mL samples were collected from each SBR throughout the return sludge treatment cycle commenced on day 94, including: (1) a mixed liquor sample immediately preceding bulk mixed liquor removal for return sludge treatment; (2) a return sludge sample after 15 min of side-stream treatment (S1); and (3) a return sludge sample after 24 h of side-stream treatment (S2). The treated return sludge samples were volume-corrected for the thickening process to attain the same biomass concentrations as the mixed liquor samples. Samples were washed in phosphate buffered saline (1x PBS; filter sterilized) through centrifugation (3000 rpm, 5 min) and resuspension to remove residual growth substrates. All samples were incubated in a media consisting of 25% synthetic wastewater in 1x PBS (vol/vol) without COD or yeast extract, so that NH_4^+-N was the only exogenous electron donor. For BONCAT-labeling microcosms, 15 mL portions of each sample were resuspended in 15 mL of incubation media amended with 1 mM homopropargylglycine (HPG; Click Chemistry Tools, USA) (HPG-positive microcosm), transferred into sterile 125 mL Erlenmeyer flasks, and incubated on an orbital shaker for 3 h at 20 °C and 200 rpm. Control microcosms (HPG-negative) for each sample were conducted similarly except without HPG amendment. Following incubations, microcosm samples were washed three times in 1x PBS to remove unincorporated HPG, resuspended in 10% (vol/vol) glycerol in PBS, aliquoted into 1 mL and stored at -80°C until further processing. Details on preliminary BONCAT validation microcosms are provided in the Supplemental Information.

BONCAT Sample Preparation and Click-Chemistry

For each microcosm type (R, S1, or S2) for both SBRs, sample preparation and click-chemistry were conducted using triplicate HPG-positive and duplicate HPG-negative microcosm samples.

Samples were thawed on ice at 4°C, enzymatically homogenized, subjected to filter-immobilized click-chemistry labeling with the FAM picolyl azide dye (Click Chemistry Tools, USA) closely following the procedure of Couradeau et al. (45), detached from the filter, pre-strained through a 30 um mesh filter, and counterstained with SYTO59 (10,000x final dilution; ThermoFisher Scientific, USA) to generate the pre-sort samples for FACS. Details of the sample homogenization and click-chemistry labeling procedures are provided in the Supplemental Information.

Fluorescence-activated cell sorting (FACS)

Fluorescence-activated cell sorting was conducted on a BD FACSJazz™ cell sorter (BD Biosciences, USA) calibrated to detect the FAM picolyl azide dye (excitation = 490 nm/emission = 510 nm) and the SYTO59 counterstain dye (excitation = 622 nm/emission = 645 nm). An overview of the FACS gating procedures is provided in the Supplemental Information. Briefly, initial gating was established with side-scatter, forward-scatter and trigger pulse width to exclude large particles and cell aggregates. Sorting gates were set targeting BONCAT-positive (BONCAT+) cell fractions based on background SYTO59 and FAM fluorescence, allowing less than 0.5% of false positives (Figures S13-S14). A total of 100k cells were analyzed from each sample, where cells within the sorting gate (SYTO+, BONCAT+) were sorted into 1.5 mL tubes containing 400 µL of prepGEM Wash Buffer (ZyGEM™, USA), and stored at -80 °C until further analysis.

DNA Extraction and 16S rRNA gene amplicon sequencing

For time-series analysis of community composition, triplicate 980 µL aliquots of mixed liquor were routinely collected directly from the SBRs at the end of a cycle and flash frozen at -80°C. Mixed liquor samples were thawed on ice, and DNA was extracted using the FastDNA Spin Kit for Soil (MP Biomedicals, USA) with minor modifications (69). For each HPG-positive microcosm type (R,

S1, or S2) for both SBRs, 50 µL aliquots were collected from the triplicate pre-homogenized and post-homogenized samples during preparation for FACS, added to 400 µL of prepGEM Wash Buffer, and stored at -80°C. Pre-homogenized samples from HPG-negative R microcosms and bulk mixed liquor samples were prepared similarly. All pre-homogenized, post-homogenized, and BONCAT-FACS samples were extracted using the prepGEM Bacteria kit (ZyGEM™) using a low-biomass input procedure overviewed in the Supplementary Information. DNA concentrations were measured with the Qubit® dsDNA BR and HS Assay Kits and Qubit® fluorometer (ThermoFisher Scientific, USA).

16S rRNA gene fragments from all DNA extracts were amplified using barcoded primers, 515F and 926R (70), targeting the V4-V5 hypervariable region of the 16S rRNA gene. All samples extracted with the prepGEM kit underwent an initial round of 15-cycles of PCR with non-barcoded 515F and 926R primers due to the low-biomass input. One triplicate set of FastDNA extracts from day 94 were also pre-amplified to determine potential biases of that step. Amplified barcoded PCR products were pooled at equimolar concentrations and sequenced on an Illumina MiSeq in paired-end 300 bp mode at the UBC Biofactorial facility.

Amplicon reads were processed and denoised into amplicon sequencing variants (ASVs) with DADA2 (49) (v.1.12.1) in the R environment. The script used to generate the ASV datasets is provided in Supplemental Information. Denoised sequences were taxonomically classified using the RDB Classifier (71) against the MiDAS 3.0 database (69).

Statistical analysis

Comparisons of reactor nutrient data were performed with t-tests for N-of-1 trials with serial correlation (72). Amplicon sequencing data was visualized using the tidyverse package (73) (v.1.3.0) in the R environment. Principal coordinates analysis (PCoA) of cumulative-sum scaled

667 (CSS) ASV read counts was performed using the metagenomeSeq (74) (v.1.26.3) and vegan (75)
668 (v.2.5.6) packages in R. PERMANOVA (adonis) was conducted in vegan with 1000 permutations
669 to determine significant differences in reactor communities over time. Differential abundance
670 analysis of ASVs between SBRs and in BONCAT microcosm datasets was performed using
671 DESeq2 (76) (v.1.24.0) using parametric fitting, the Wald significance test, and Benjamin-
672 Hochberg correction for *p* values. A $\log_2$-fold change of an ASV represents the multiplicative effect
673 size for changes in normalized read counts across treatments on a logarithmic scale to base 2.
674 Sequence similarity values between ASVs were calculated using the NCBI Basic Local Alignment
675 Search Tool (77). FACS data was processed using the flowcore package (v.1.52.1) (78) in R.
676
677 **Data Availability**
678 The raw read files of 16S rRNA gene amplicons are available via the NCBI Short Read Archive
679 under BioProject PRJNA693634.
680
681
682 **Acknowledgements**
683 This work was supported by the Natural Sciences and Engineering Research Council (NSERC)
684 of Canada (Discovery Grant). MM was supported by an NSERC CGS-M fellowship.
685
686 **Author Information**
687 MM and YL contributed equally to this work.
688

689 **References**

690

691 1. Leggieri PA, Liu Y, Hayes M, Connors B, Seppälä S, O'Malley MA, Venturelli OS. 2021.
692 Integrating Systems and Synthetic Biology to Understand and Engineer Microbiomes.
693 Annu Rev Biomed Eng 23:annurev-bioeng-082120-022836.
694 2. Lawson CE, Harcombe WR, Hatzenpichler R, Lindemann SR, Löffler FE, O'Malley MA,
695 García Martín H, Pfleger BF, Raskin L, Venturelli OS, Weissbrodt DG, Noguera DR,
696 McMahon KD. 2019. Common principles and best practices for engineering microbiomes.
697 Nat Rev Microbiol 17:725–741.
698 3. Verstraete W, Wittebolle L, Heylen K, Vanparys B, de Vos P, van de Wiele T, Boon N.
699 2007. Microbial Resource Management: The Road To Go for Environmental
700 Biotechnology. Eng Life Sci 7:117–126.
701 4. Daims H, Taylor MW, Wagner M. 2006. Wastewater treatment: a model system for
702 microbial ecology. Trends Biotechnol 24:483–489.
703 5. Cogert KI, Ziels RM, Winkler MKH. 2019. Reducing Cost and Environmental Impact of
704 Wastewater Treatment with Denitrifying Methanotrophs, Anammox, and Mainstream
705 Anaerobic Treatment. Environ Sci Technol 53:12935–12944.
706 6. McCarty PL, Bae J, Kim J. 2011. Domestic Wastewater Treatment as a Net Energy
707 Producer–Can This be Achieved? Environ Sci Technol 45:7100–7106.
708 7. Drewnowski J, Remiszewska-Skwarek A, Duda S, Łagód G. 2019. Aeration Process in
709 Bioreactors as the Main Energy Consumer in a Wastewater Treatment Plant. Review of
710 Solutions and Methods of Process Optimization. Processes 7:311.
711 8. Li X, Klaus S, Bott C, He Z. 2018. Status, Challenges, and Perspectives of Mainstream
712 Nitritation-Anammox for Wastewater Treatment. Water Environ Res 90:634–649.
713 9. Agrawal S, Seuntjens D, Cocker PD, Lackner S, Vlaeminck SE. 2018. Success of
714 mainstream partial nitritation/anammox demands integration of engineering, microbiome

715 and modeling insights. Curr Opin Biotechnol 50:214–221.
716 10. Kartal B, Kuenen JG, van Loosdrecht MCM. 2010. Sewage Treatment with Anammox.
717 Science 328:702–703.
718 11. Tang C-J, Zheng P, Chai L-Y, Min X-B. 2013. Thermodynamic and kinetic investigation of
719 anaerobic bioprocesses on ANAMMOX under high organic conditions. Chem Eng J
720 230:149–157.
721 12. Turk O, Mavinic DS. 1986. Preliminary assessment of a shortcut in nitrogen removal from
722 wastewater. Can J Civ Eng 13:600–605.
723 13. Regmi P, Miller MW, Holgate B, Bunce R, Park H, Chandran K, Wett B, Murthy S, Bott CB.
724 2014. Control of aeration, aerobic SRT and COD input for mainstream
725 nitritation/denitritation. Water Res 57:162–171.
726 14. Xu G, Zhou Y, Yang Q, Lee ZM-P, Gu J, Lay W, Cao Y, Liu Y. 2015. The challenges of
727 mainstream deammonification process for municipal used water treatment. Appl Microbiol
728 Biotechnol 99:2485–2490.
729 15. Cao Y, Loosdrecht MCM van, Daigger GT. 2017. Mainstream partial nitritation–anammox
730 in municipal wastewater treatment: status, bottlenecks, and further studies. Appl Microbiol
731 Biotechnol 101:1365–1383.
732 16. Ge S, Peng Y, Qiu S, Zhu A, Ren N. 2014. Complete nitrogen removal from municipal
733 wastewater via partial nitrification by appropriately alternating anoxic/aerobic conditions in
734 a continuous plug-flow step feed process. Water Res 55:95–105.
735 17. Kornaros M, Dokianakis SN, Lyberatos G. 2010. Partial Nitrification/Denitrification Can Be
736 Attributed to the Slow Response of Nitrite Oxidizing Bacteria to Periodic Anoxic
737 Disturbances. Environ Sci Technol 44:7245–7253.
738 18. Vadivelu VM, Keller J, Yuan Z. 2007. Free ammonia and free nitrous acid inhibition on the
739 anabolic and catabolic processes of Nitrosomonas and Nitrobacter. Water Sci Technol
740 56:89–97.

741 19. Park S, Bae W. 2009. Modeling kinetics of ammonium oxidation and nitrite oxidation under
742 simultaneous inhibition by free ammonia and free nitrous acid. Process Biochem 44:631–
743 640.
744 20. Vadivelu VM, Keller J, Yuan Z. 2007. Effect of free ammonia on the respiration and growth
745 processes of an enriched Nitrobacter culture. Water Res 41:826–834.
746 21. Wang Q, Duan H, Wei W, Ni B-J, Laloo A, Yuan Z. 2017. Achieving Stable Mainstream
747 Nitrogen Removal via the Nitrite Pathway by Sludge Treatment Using Free Ammonia.
748 Environ Sci Technol 51:9800–9807.
749 22. Wang D, Wang Q, Laloo A, Xu Y, Bond PL, Yuan Z. 2016. Achieving Stable Nitritation for
750 Mainstream Deammonification by Combining Free Nitrous Acid-Based Sludge Treatment
751 and Oxygen Limitation. Sci Rep 6:25547.
752 23. Wang Q, Ye L, Jiang G, Hu S, Yuan Z. 2014. Side-stream sludge treatment using free
753 nitrous acid selectively eliminates nitrite oxidizing bacteria and achieves the nitrite
754 pathway. Water Res 55:245–255.
755 24. Daims H, Lücker S, Wagner M. 2016. A New Perspective on Microbes Formerly Known as
756 Nitrite-Oxidizing Bacteria. Trends Microbiol 24:699–712.
757 25. Lücker S, Schwarz J, Gruber-Dorninger C, Spieck E, Wagner M, Daims H. 2015.
758 Nitrotoga-like bacteria are previously unrecognized key nitrite oxidizers in full-scale
759 wastewater treatment plants. ISME J 9:708–720.
760 26. Spasov E, Tsuji JM, Hug LA, Doxey AC, Sauder LA, Parker WJ, Neufeld JD. 2019. High
761 functional diversity among *Nitrospira* populations that dominate rotating biological
762 contactor microbial communities in a municipal wastewater treatment plant. preprint,
763 Microbiology.
764 27. Yang Y, Daims H, Liu Y, Herbold CW, Pjevac P, Lin J-G, Li M, Gu J-D. 2020. Activity and
765 Metabolic Versatility of Complete Ammonia Oxidizers in Full-Scale Wastewater Treatment
766 Systems. mBio 11:e03175-19, /mbio/11/2/mBio.03175-19.atom.

767 28. Camejo PY, Santo Domingo J, McMahon KD, Noguera DR. 2017. Genome-Enabled
768 Insights into the Ecophysiology of the Comammox Bacterium " *Candidatus* Nitrospira
769 nitrosa." mSystems 2.
770 29. Sorokin DY, Lücker S, Vejmelkova D, Kostrikina NA, Kleerebezem R, Rijpstra WIC,
771 Damsté JSS, Le Paslier D, Muyzer G, Wagner M, van Loosdrecht MCM, Daims H. 2012.
772 Nitrification expanded: discovery, physiology and genomics of a nitrite-oxidizing bacterium
773 from the phylum Chloroflexi. ISME J 6:2245–2256.
774 30. Nowka B, Daims H, Spieck E. 2015. Comparison of Oxidation Kinetics of Nitrite-Oxidizing
775 Bacteria: Nitrite Availability as a Key Factor in Niche Differentiation. Appl Environ Microbiol
776 81:745–753.
777 31. Nogueira R, Melo LF. 2006. Competition betweenNitrospira spp. andNitrobacter spp. in
778 nitrite-oxidizing bioreactors. Biotechnol Bioeng 95:169–175.
779 32. Global Water Microbiome Consortium, Wu L, Ning D, Zhang B, Li Y, Zhang P, Shan X,
780 Zhang Q, Brown MR, Li Z, Van Nostrand JD, Ling F, Xiao N, Zhang Y, Vierheilig J, Wells
781 GF, Yang Y, Deng Y, Tu Q, Wang A, Zhang T, He Z, Keller J, Nielsen PH, Alvarez PJJ,
782 Criddle CS, Wagner M, Tiedje JM, He Q, Curtis TP, Stahl DA, Alvarez-Cohen L, Rittmann
783 BE, Wen X, Zhou J. 2019. Global diversity and biogeography of bacterial communities in
784 wastewater treatment plants. Nat Microbiol 4:1183–1195.
785 33. Daims H, Nielsen JL, Nielsen PH, Schleifer K-H, Wagner M. 2001. In Situ Characterization
786 of Nitrospira-Like Nitrite-Oxidizing Bacteria Active in Wastewater Treatment Plants. Appl
787 Environ Microbiol 67:5273–5284.
788 34. Gruber-Dorninger C, Pester M, Kitzinger K, Savio DF, Loy A, Rattei T, Wagner M, Daims
789 H. 2015. Functionally relevant diversity of closely related Nitrospira in activated sludge.
790 ISME J 9:643–655.
791 35. Maixner F, Noguera DR, Anneser B, Stoecker K, Wegl G, Wagner M, Daims H. 2006.
792 Nitrite concentration influences the population structure of Nitrospira-like bacteria. Environ

Microbiol 8:1487–1495.

36. Hee-Deung P, Daniel R. Noguera. 2008. Nitrospira community composition in nitrifying reactors operated with two different dissolved oxygen levels. J Microbiol Biotechnol 18:1470–1474.

37. Koch H, Lücker S, Albertsen M, Kitzinger K, Herbold C, Spieck E, Nielsen PH, Wagner M, Daims H. 2015. Expanded metabolic versatility of ubiquitous nitrite-oxidizing bacteria from the genus Nitrospira. Proc Natl Acad Sci 112:11371–11376.

38. Koch H, Galushko A, Albertsen M, Schintlmeister A, Gruber-Dorninger C, Lücker S, Pelletier E, Paslier DL, Spieck E, Richter A, Nielsen PH, Wagner M, Daims H. 2014. Growth of nitrite-oxidizing bacteria by aerobic hydrogen oxidation. Science 345:1052–1054.

39. Lucker S, Wagner M, Maixner F, Pelletier E, Koch H, Vacherie B, Rattei T, Damste JSS, Spieck E, Le Paslier D, Daims H. 2010. A Nitrospira metagenome illuminates the physiology and evolution of globally important nitrite-oxidizing bacteria. Proc Natl Acad Sci 107:13479–13484.

40. Ushiki N, Jinno M, Fujitani H, Suenaga T, Terada A, Tsuneda S. 2017. Nitrite oxidation kinetics of two Nitrospira strains: The quest for competition and ecological niche differentiation. J Biosci Bioeng 123:581–589.

41. Duan H, Ye L, Lu X, Yuan Z. 2019. Overcoming Nitrite Oxidizing Bacteria Adaptation through Alternating Sludge Treatment with Free Nitrous Acid and Free Ammonia. Environ Sci Technol 53:1937–1946.

42. Li S, Duan H, Zhang Y, Huang X, Yuan Z, Liu Y, Zheng M. 2020. Adaptation of nitrifying community in activated sludge to free ammonia inhibition and inactivation. Sci Total Environ 728:138713.

43. Liu G, Wang J. 2013. Long-Term Low DO Enriches and Shifts Nitrifier Community in Activated Sludge. Environ Sci Technol 47:5109–5117.

819 44. Hatzenpichler R, Krukenberg V, Spietz RL, Jay ZJ. 2020. Next-generation physiology
820 approaches to study microbiome function at single cell level. Nat Rev Microbiol
821 https://doi.org/10.1038/s41579-020-0323-1.
822 45. Couradeau E, Sasse J, Goudeau D, Nath N, Hazen TC, Bowen BP, Chakraborty R,
823 Malmstrom RR, Northen TR. 2019. Probing the active fraction of soil microbiomes using
824 BONCAT-FACS. Nat Commun 10:2770.
825 46. Hatzenpichler R, Connon SA, Goudeau D, Malmstrom RR, Woyke T, Orphan VJ. 2016.
826 Visualizing in situ translational activity for identifying and sorting slow-growing
827 archaeal−bacterial consortia. Proc Natl Acad Sci 113:E4069–E4078.
828 47. Hatzenpichler R, Scheller S, Tavormina PL, Babin BM, Tirrell DA, Orphan VJ. 2014. *In situ*
829 visualization of newly synthesized proteins in environmental microbes using amino acid
830 tagging and click chemistry: Visualizing new proteins in microbes by click chemistry.
831 Environ Microbiol 16:2568–2590.
832 48. Reichart NJ, Jay ZJ, Krukenberg V, Parker AE, Spietz RL, Hatzenpichler R. 2020. Activity-
833 based cell sorting reveals responses of uncultured archaea and bacteria to substrate
834 amendment. ISME J https://doi.org/10.1038/s41396-020-00749-1.
835 49. Callahan BJ, McMurdie PJ, Rosen MJ, Han AW, Johnson AJA, Holmes SP. 2016. DADA2:
836 High-resolution sample inference from Illumina amplicon data. Nat Methods 13:581–583.
837 50. Eren AM, Morrison HG, Lescault PJ, Reveillaud J, Vineis JH, Sogin ML. 2015. Minimum
838 entropy decomposition: Unsupervised oligotyping for sensitive partitioning of high-
839 throughput marker gene sequences. 4. ISME J 9:968–979.
840 51. Nowka B, Off S, Daims H, Spieck E. 2015. Improved isolation strategies allowed the
841 phenotypic differentiation of two Nitrospira strains from widespread phylogenetic lineages.
842 FEMS Microbiol Ecol 91.
843 52. Daims H, Lebedeva EV, Pjevac P, Han P, Herbold C, Albertsen M, Jehmlich N,
844 Palatinszky M, Vierheilig J, Bulaev A, Kirkegaard RH, von Bergen M, Rattei T, Bendinger

B, Nielsen PH, Wagner M. 2015. Complete nitrification by Nitrospira bacteria. 7583. Nature 528:504–509.

53. Wright E S. 2016. Using DECIPHER v2.0 to Analyze Big Biological Sequence Data in R. R J 8:352.

54. Schliep KP. 2011. phangorn: phylogenetic analysis in R. Bioinformatics 27:592–593.

55. Daebeler A, Kitzinger K, Koch H, Herbold CW, Steinfeder M, Schwarz J, Zechmeister T, Karst SM, Albertsen M, Nielsen PH, Wagner M, Daims H. 2020. Exploring the upper pH limits of nitrite oxidation: diversity, ecophysiology, and adaptive traits of haloalkalitolerant Nitrospira. 12. ISME J 14:2967–2979.

56. Sánchez O, Aspé E, Martí MC, Roeckel M. 2004. The Effect of Sodium Chloride on the Two–Step Kinetics of the Nitrifying Process. Water Environ Res 76:73–80.

57. Turk O, Mavinic DS. 1989. Stability of Nitrite Build-Up in an Activated Sludge System. J Water Pollut Control Fed 61:1440–1448.

58. Blackburne R, Vadivelu VM, Yuan Z, Keller J. 2007. Kinetic characterisation of an enriched Nitrospira culture with comparison to Nitrobacter. Water Res 41:3033–3042.

59. Wegen S, Nowka B, Spieck E. 2019. Low Temperature and Neutral pH Define “Candidatus Nitrotoga sp.” as a Competitive Nitrite Oxidizer in Coculture with Nitrospira defluvii. Appl Environ Microbiol 85.

60. Bayer B, Saito MA, McIlvin MR, Lücker S, Moran DM, Lankiewicz TS, Dupont CL, Santoro AE. 2021. Metabolic versatility of the nitrite-oxidizing bacterium Nitrospira marina and its proteomic response to oxygen-limited conditions. ISME J 15:1025–1039.

61. Louca S, Polz MF, Mazel F, Albright MBN, Huber JA, O’Connor MI, Ackermann M, Hahn AS, Srivastava DS, Crowe SA, Doebeli M, Parfrey LW. 2018. Function and functional redundancy in microbial systems. Nat Ecol Evol 2:936–943.

62. Henze M, Gujer W, Mino T, Loosdrecht MCM van. 2000. Activated sludge models ASM1, ASM2, ASM2d and ASM3. IWA Publishing.

871 63. Metcalf & Eddy, Inc., Tchobanoglous G, Burton F, Stensel HD. 2014. Wastewater
872 Engineering: Treatment and Resource Recovery, 5th ed. McGraw-Hill.
873 64. Louca S, Hawley AK, Katsev S, Torres-Beltran M, Bhatia MP, Kheirandish S, Michiels CC,
874 Capelle D, Lavik G, Doebeli M, Crowe SA, Hallam SJ. 2016. Integrating biogeochemistry
875 with multiomic sequence information in a model oxygen minimum zone. Proc Natl Acad Sci
876 113:E5925–E5933.
877 65. Reed DC, Algar CK, Huber JA, Dick GJ. 2014. Gene-centric approach to integrating
878 environmental genomics and biogeochemical models. Proc Natl Acad Sci 111:1879–1884.
879 66. Nielsen PH, Mielczarek AT, Kragelund C, Nielsen JL, Saunders AM, Kong Y, Hansen AA,
880 Vollertsen J. 2010. A conceptual ecosystem model of microbial communities in enhanced
881 biological phosphorus removal plants. Water Res 44:5070–5088.
882 67. Ziels RM, Svensson BH, Sundberg C, Larsson M, Karlsson A, Yekta SS. 2018. Microbial
883 rRNA gene expression and co-occurrence profiles associate with biokinetics and elemental
884 composition in full-scale anaerobic digesters. Microb Biotechnol 11:694–709.
885 68. Jeong SY, Chang SW, Ngo HH, Guo W, Nghiem LD, Banu JR, Jeon B-H, Nguyen DD.
886 2019. Influence of thermal hydrolysis pretreatment on physicochemical properties and
887 anaerobic biodegradability of waste activated sludge with different solids content. Waste
888 Manag 85:214–221.
889 69. Nierychlo M, Andersen KS, Xu Y, Green N, Jiang C, Albertsen M, Dueholm MS, Nielsen
890 PH. 2020. MiDAS 3: An ecosystem-specific reference database, taxonomy and knowledge
891 platform for activated sludge and anaerobic digesters reveals species-level microbiome
892 composition of activated sludge. Water Res 115955.
893 70. Parada AE, Needham DM, Fuhrman JA. 2016. Every base matters: assessing small
894 subunit rRNA primers for marine microbiomes with mock communities, time series and
895 global field samples. Environ Microbiol 18:1403–1414.
896 71. Wang Q, Garrity GM, Tiedje JM, Cole JR. 2007. Naïve Bayesian Classifier for Rapid

Assignment of rRNA Sequences into the New Bacterial Taxonomy. Appl Environ Microbiol 73:5261–5267.

72. Tang J, Landes RD. 2020. Some t-tests for N-of-1 trials with serial correlation. PLOS ONE 15:e0228077.

73. Wickham H, Averick M, Bryan J, Chang W, McGowan LD, François R, Grolemund G, Hayes A, Henry L, Hester J, Kuhn M, Pedersen TL, Miller E, Bache SM, Müller K, Ooms J, Robinson D, Seidel DP, Spinu V, Takahashi K, Vaughan D, Wilke C, Woo K, Yutani H. 2019. Welcome to the Tidyverse. J Open Source Softw 4:1686.

74. Paulson JN, Stine OC, Bravo HC, Pop M. 2013. Differential abundance analysis for microbial marker-gene surveys. 12. Nat Methods 10:1200–1202.

75. Oksanen J, Kindt R, Legendre P, O'Hara B, Stevens MHH, Oksanen MJ, Suggests M. 2007. The vegan package. Community Ecol Package 10:719.

76. Love MI, Huber W, Anders S. 2014. Moderated estimation of fold change and dispersion for RNA-seq data with DESeq2. Genome Biol 15:550.

77. Altschul SF, Gish W, Miller W, Myers EW, Lipman DJ. 1990. Basic local alignment search tool. J Mol Biol 215:403–410.

78. Hahne F, LeMeur N, Brinkman RR, Ellis B, Haaland P, Sarkar D, Spidlen J, Strain E, Gentleman R. 2009. flowCore: a Bioconductor package for high throughput flow cytometry. BMC Bioinformatics 10:106.